Tyr275 and Lys279 Stabilize NADPH within the Catalytic Site of NADPH:Protochlorophyllide Oxidoreductase and Are Involved in the Formation of the Enzyme Photoactive State†

Nikolai Lebedev,* Olga Karginova, Wilson McIvor, and Michael P. Timko

Department of Biology, University of Virginia, Charlottesville, Virginia 22903

Received March 12, 2001; Revised Manuscript Received August 15, 2001

ABSTRACT: Fluorescence spectroscopic and kinetic analysis of photochemical activity, cofactor and substrate binding, and enzyme denaturation studies were performed with highly purified, recombinant pea NADPH: protochlorophyllide oxidoreductase (POR) heterologously expressed in *Escherichia coli*. The results obtained with an individual stereoisomer of the substrate [C8-ethyl-C13(2)-(*R*)-protochlorophyllide] demonstrate that the enzyme photoactive state possesses a characteristic fluorescence maximum at 646 nm that is due to the presence of specific charged amino acids in the enzyme catalytic site. The photoactive state is converted directly into an intermediate having fluorescence at 685 nm in a reaction involving direct hydrogen transfer from the cofactor (NADPH). Site-directed mutagenesis of the highly conserved Tyr275 (Y275F) and Lys279 (K279I and K279R) residues in the enzyme catalytic pocket demonstrated that the presence of these two amino acids in the wild-type POR considerably increases the probability of photoactive state formation following cofactor and substrate binding by the enzyme. At the same time, the presence of these two amino acids destabilizes POR and increases the rate of enzyme denaturation. Neither Tyr275 nor Lys279 plays a crucial role in the binding of the substrate or cofactor by the enzyme. In addition, the presence of Tyr275 is absolutely necessary for the second step of the protochlorophyllide reduction reaction, "dark" conversion of the 685 nm fluorescence intermediate and the formation of the final product, chlorophyllide. We propose that Tyr275 and Lys279 participate in the proper coordination of NADPH and PChlide in the enzyme catalytic site and thereby control the efficiency of the formation of the POR photoactive state.

NADPH:protochlorophyllide oxidoreductase (POR,[1] EC 1.6.99.1) catalyzes hydrogen transfer from NADPH to PChlide in the course of chlorophyll biosynthesis in higher plants, algae, and cyanobacteria. A unique feature of this enzyme is the direct regulation of its catalytic activity by light (*1*). The light dependency of the enzyme distinguishes it from all other known oxidoreductases and makes it very attractive for the construction of artificial photoregulated enzymatic systems. Prior investigation of the enzyme's properties led to the discovery of several important features of the POR catalytic mechanism. Studies with cofactor analogues clearly showed that NADPH but not NADH can serve as a cofactor in the reaction (*2*). NADPH binding by the enzyme protects one or more of the conserved Cys residues in the enzyme from chemical modification (*3*). Using isotope-labeled NADPH derivatives, it was also shown that only the 4(*S*)-hydrogen of NADPH is transferred to the pigment in the course of the reaction (*4*) and that the transfer is to the C17 atom of the porphyrin (*5*). Studies with different porphyrin derivatives led to the conclusion that PChlide interacts with the enzyme through the metal atom (*6*) and C13[2] side chain group (*7*). It also appears that the C7 and C8 positions on the porphyrin ring do not participate directly in the reaction, since neither an ethyl to vinyl substitution at the C8 position (*8*) nor a methyl to formyl group change at C7 of the porphyrin ring affects POR activity (*9*, *10*).

The cloning and characterization of cDNAs and nuclear genes encoding POR (*11*−*13*) provided critically needed information about primary structure and has subsequently contributed to our better understanding of enzyme structure−function relationships (*14*). Comparisons of the amino acid sequence of POR with those present in the various protein and nucleic acid sequence databases led to the recognition that POR belongs to a large family of short chain dehydrogenases/reductases termed the SDR family (*1*, *15*). Members of the SDR family of enzymes have many structural features in common, including conserved cofactor (NADH/NADPH) binding domains encompassing a $\beta-\alpha-\beta$ fold and active sites with highly conserved Tyr and Lys residues separated

† This work was supported by the U.S. Department of Energy (DEFGO5-94ER20144).

* To whom correspondence should be addressed. Present address: Center for Biomolecular Science and Engineering, Code 6900, U.S. Naval Research Laboratory, 4555 Overlook Ave., SW, Washington, DC 20375-5348. E-mail: ln4u@virginia.edu. Fax: (202) 404-8897. Telephone: (202) 404-6073.

[1] Abbreviations: AKR, aldoketoreductases; CD, circular dichroism; Chlide, chlorophyllide; DV-PChlide, C8-vinyl-PChlide; E*X*, excitation maximum at *X* nm; IPTG, isopropyl β-D-thiogalactoside; F*X*, fluorescence maximum at *X* nm; HPLC, high-performance liquid chromatography; MBP, maltose-binding protein; β-ME, β-mercaptoethanol; MV-PChlide, C8-ethyl-PChlide; PChlide, protochlorophyllide; POR, NADPH: protochlorophyllide oxidoreductase; SDR, short chain dehydrogenase/reductase; SDS−PAGE, sodium dodecyl sulfate−polyacrylamide gel electrophoresis; WT, wild type.

10.1021/bi0105025 CCC: $20.00
Published on Web 09/29/2001

by three amino acids (*16*). Site-directed mutagenesis studies have established that these conserved Tyr and Lys residues are absolutely necessary for the enzyme catalytic activity (*17*, *18*). Although the exact role of these residues in enzyme function is not known, Wilks and Timko (*15*) have suggested that Tyr275 in POR participates directly in catalysis by contributing the hydrogen for transfer to the pigment.

A large amount of information is available on the nature of cofactor binding domains and the process of NADH/NADPH binding in various SDR family members, providing some comparative insight into cofactor binding in POR. In contrast, no sequence similarity exists between POR and other chlorophyll-binding proteins (in particular, the light-harvesting and reaction center proteins of the photosynthetic apparatus) which might provide information about the nature of the pigment binding site in POR. To address the lack of information about POR catalytic domains, a charged-to-alanine scanning mutagenesis study of the pea POR was carried out (*14*). These studies led to the identification of several domains within the enzyme that are required for catalytic activity and might be important in POR−PChlide interaction.

Recent studies with heterologously overexpressed POR fusion proteins have greatly facilitated the analysis of the requirements of the POR catalytic mechanism (*19*−*21*). Analysis of the dependency of the reaction on substrate and cofactor concentrations and light intensity has shown that one pigment and one NADPH molecule participate in the formation of the photoactive reaction complex and the reaction proceeds through a single-quantum mechanism (*22*, *23*). Analysis of POR activity at low temperatures led to the identification of two reaction steps, one photochemical and the other nonphotochemical, linked by the formation of an unstable fluorescent intermediate (*23*).

In this study, we introduced a new system for the analysis of POR structure and activity, using highly purified recombinant POR protein devoid of any additional sequences. Furthermore, to further clarify the role of the conserved catalytic site Tyr and Lys residues in the enzyme molecular organization and catalytic activity, we constructed several mutants of the recombinant pea POR with Y275F, K279I, and K279R substitutions. The effects of these modifications on enzyme stability and the ability to bind substrate and cofactor, to form the photoactive state, and to subsequently convert bound pigment into the 685 nm reaction intermediate and Chlide, the final product of the reaction, were assayed. Our data indicate that Tyr275 and Lys279 are responsible for coordinating the substrate and cofactor in the proper orientation in the enzyme. Their substitution does not prevent the enzyme from binding substrate and cofactor, but modifies their interaction as part of the POR−NADPH−PChlide ternary complex and considerably suppresses formation of the enzyme photoactive state. We also show that Tyr275 is necessary for the second "dark" step of PChlide photoreduction. Substitution of these residues in the POR protein does not inactivate the photoformation of the 685 nm fluorescence intermediate, but completely blocks its conversion into the final product, Chlide.

MATERIALS AND METHODS

Chemicals. Unless otherwise stated, chemicals were obtained from Fisher Scientific, J. T. Baker, or U.S. Biochemical Corp. and were analytical grade or better. Chemicals for SDS−PAGE were purchased from Bio-Rad. Analytical grade NADPH, NADH, and $NADP^+$ were purchased from Sigma. *Escherichia coli* strain ER2508 and amylose resin were from New England Biolabs. DNA restriction endonucleases, T4 DNA polymerase, DNA ligase, and DNA modification buffers were from Roche, BRL, and New England Biolabs. Enhanced chemiluminescence detection reagents and secondary antibody were from Amersham. Rabbit polyclonal antibody for the purified recombinant wheat POR was a gift from W. T. Griffiths (Department of Biochemistry, University of Bristol, Bristol, U.K.).

Construction, Expression, and Purification of WT and Mutant Pea POR Proteins. The cloning of the WT pea POR cDNA and construction of mutant POR protein coding sequences containing single-site amino acid substitutions were described previously (*15*). Site-directed mutagenesis of the coding region of the mature protein of WT pea POR was carried out using the pAlter mutagenesis vector (Promega) and the manufacturer's protocol. The following oligonucleotides carrying nucleotide mismatches (bold) were used to direct the synthesis of the mutant genes: 5′-tggtgccaaggc**ctt**caaggacag (Y275F), 5′-ggcatacaaggac**tcg**a**tc**gtctgtaat (K279I), and 5′-ggcatacaaggac**tcgcg**agtctgtaat (K279R) (*15*). Nucleotide sequences encoding the WT and mutated pea POR proteins were cloned at the *Bam*HI and *Pst*I restriction sites in pMBPHIS, an expression vector containing the coding sequence of the bacterial maltose binding protein (MBP), six histidines, and the TEV cleavage site (*24*). The recombinant plasmids were transformed into *E. coli* ER2508, and recombinant protein overexpression was carried out as described below. The veracity of all recombinant constructs was confirmed by nucleotide sequencing (*25*).

For isolation of the recombinant POR proteins, *E. coli* cells containing the various constructs were grown in Luria broth (LB) containing 100 mg/L ampicillin and 15 mg/L tetacycline (*19*). Exponentially growing cultures were treated with 0.1 mM IPTG overnight to induce MBP−$(His)_6$−POR expression. The cells were collected by centrifugation, resuspended in extraction buffer [50 mM Tris-HCl (pH 8.0), 300 mM NaCl, and 10 mM β-ME, with 0.1% Emulgen (KARLAN Research Products Corp.)], and sonicated on ice for 90 s per each 500 mL of cells in a VirSonic 60/VirTis apparatus with an output power of 2 W. The cell debris was removed by centrifugation at 10000*g* for 20 min, and the supernatant was applied to a Ni−NTA column equilibrated with the same buffer. After a 40 min incubation, the column was washed with 10 volumes of washing buffer [50 mM Tris-HCl (pH 8.0), 300 mM NaCl, 10 mM β-ME, and 10 mM imidazole], and the proteins were eluted with buffer containing 50 mM Tris-HCl (pH 8.0), 300 mM NaCl, 10 mM β-ME, and 100 mM imidazole. Following chromatography on Ni−NTA resin, the MBP−$(His)_6$−POR fusion proteins were cleaved at the TEV site with recombinant rTEV protease (Life Technologies) using a ratio of 30 units of protease/mg of recombinant protein. The cleavage products were dialyzed against 50 mM Tris-HCl (pH 8.0), 300 mM NaCl, 5 mM β-ME, and 0.1% Emulgen for 12 h at 10 °C to remove the imidazole. Following dialysis, the protein mixture was passed over a Ni−NTA column as described above to remove the MBP−$(His)_6$ fragment and any uncleaved MBP−$(His)_6$−POR fusion protein. The column eluate was concentrated

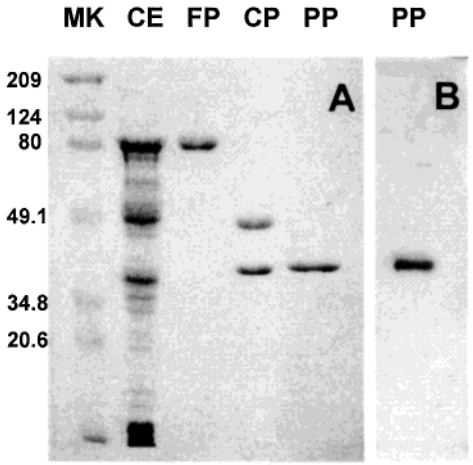

FIGURE 1: Purification of recombinant pea POR protein and its characterization by SDS−PAGE and Western blot analysis. (A) Coomassie Brilliant Blue-stained polypeptide profiles following SDS−PAGE of POR-containing fractions during various stages of purification. CE, crude *E. coli* extract after cell sonication; FP, eluate from the first Ni−NTA column chromatography; CP, fusion protein following cleavage with rTEV protease and dialysis; PP, eluate from the second Ni−NTA column chromatography after concentration in an ultra-spin column; MK, molecular mass markers. (B) Western blot of purified POR preparations identical to those shown in the last lane of panel A. All data shown were prepared using the WT POR.

by filtration through a Centicon YM10 (Millipore) column and dialyzed against 50 mM Tris-HCl (pH 8.0), 300 mM NaCl, and 5 mM β-ME for 6−8 h at 10 °C to remove the detergent. The recombinant POR proteins obtained using this procedure are 95% pure as determined by SDS−PAGE (Figure 1) and have a predicted molecular mass of 36 kDa.

The protein concentration in the samples was determined as previously described (*26*). For SDS−PAGE, the samples were diluted with electrophoresis sample buffer [final concentrations of 70 mM Tris-HCl (pH 6.8), 1% (w/v) SDS, 7% (v/v) glycerol, 1.5% (v/v) β-ME, and 0.03% (w/v) bromphenol blue], aliquots were heat denatured (95 °C, 3 min), and the proteins were fractionated on 8% (w/v) polyacrylamide gels (*3*, *27*). Following electrophoresis, either the gels were stained with Coomassie Brilliant Blue R-250 to visualize the proteins or the proteins were electrophoretically blotted to Protran BA83 nitrocellulose membrane (Schleicher & Schuell) for immunological analysis. Immunological detection of POR was performed using polyclonal antiserum raised against purified recombinant wheat POR (kindly provided by W. T. Griffiths) in conjunction with the enhanced chemiluminescence detection kit (Amersham) (*27*).

Protochlorophyllide Isolation, Purification, and Identification. PChlide was isolated from dark-grown cultures of *Rhodobacter capsulatus* strain ZY5, a mutant of the purple non-sulfur bacterium carrying a mutation in the bchL subunit of the PChlide-reducing enzyme and completely unable to reduce PChlide into Chlide (*15*). Bacterial cultures were grown in liquid RCV+ medium containing 25 μg/mL rifampicin for 2 days at 28−32 °C with constant shaking (200 rpm). At the logarithmic phase of growth, the cells were collected by centrifugation and the pigments extracted with ice-cold 100% acetone. The pigments from the concentrated extract were separated isocratically on a reverse-phase C8 column (4.6 mm × 250 mm, Vydac) in a 52% (v/v) acetone/

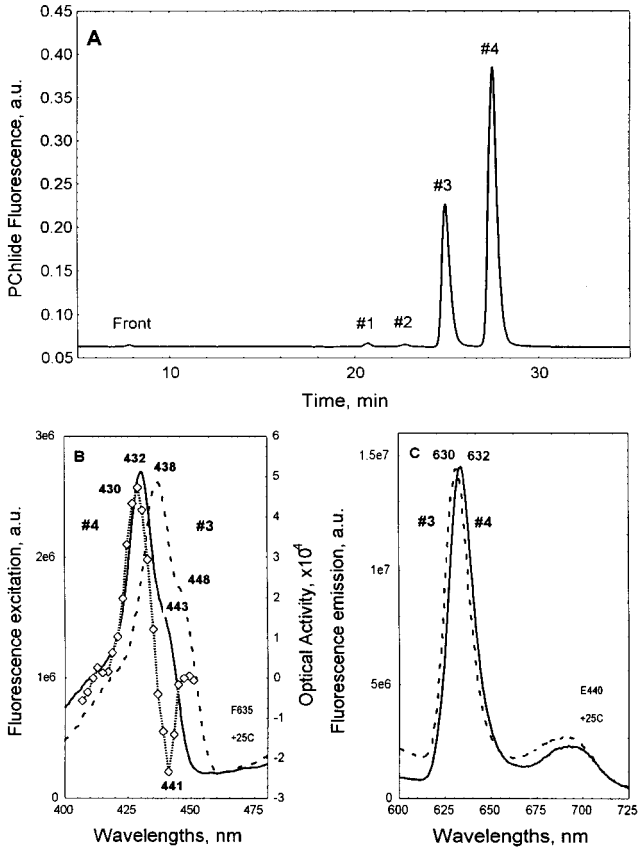

FIGURE 2: HPLC purification of PChlides and their identification by fluorescence emission, excitation, and CD spectra. (A) HPLC profile of four pigment fractions detected in the acetone extract of *R. capsulatus* ZY5 cells after isocratic separation in an acetone/water mixture. Fluorescence excitation and emission wavelengths used for pigment monitoring were 435 and 635 nm, respectively. (B) Fluorescence excitation and CD spectra of the pigment present in HPLC fractions 3 and 4 in diethyl ether. Only CD spectrum for fraction 4 is shown. (C) Fluorescence emission spectra of the pigment present in HPLC fractions 3 and 4 in diethyl ether.

water solution at a flow rate of 1 mL/min at room temperature using a Beckman System Gold HPLC apparatus equipped with an Intelligent Jasco FP-920 fluorescence detector. Four fractions containing PChlide were detected and collected by monitoring fluorescence at 635 nm under excitation at 435 nm (Figure 2A). The acetone was evaporated from the various fractions under a flow of argon; the pigments were extracted from the remaining water phase with diethyl ether, assayed for their fluorescence excitation, emission, and CD spectra, and crystallized by evaporation of the ether at room temperature. The first two HPLC fractions had fluorescence maxima in diethyl ether at 629 and 631 nm with corresponding excitation maxima at 437 and 432 nm, respectively. The other two fractions had fluorescence maxima at 630 and 632 nm with corresponding excitation maxima at 438 and 432 nm, respectively (Figure 2B,C). The CD activity of fraction 3 was positive at 438 nm and negative at 448 nm bands. The CD activity of fraction 4 was positive at 432 nm and negative at 443 nm bands. Aliquots of the crystallized pigment were stored at −20 °C and used in the various experiments described below after solubilization in methanol.

Spectroscopic Analysis of Pigment, NADPH, and POR Protein at Ambient and Low Temperatures. For fluorescence

measurements, photoactive POR complexes were formed in a reaction buffer containing 50 mM Tris-HCl (pH 8.0), 300 mM NaCl, and 10 mM β-ME. Where indicated, 0.01 or 0.1% Triton X-100 (final concentration) was added. The standard concentrations used in kinetic experiments were 100 nM recombinant protein, 20 nM PChlide, and 1 μM NADPH, unless indicated otherwise. The reaction mixture was prepared under green safe light and allowed to equilibrate at room temperature (25 °C) in the dark for 5 min. Samples were either used for room-temperature fluorescence assays or placed on a sample holder and quickly frozen in liquid nitrogen. Low-temperature spectra were recorded at narrow angles with a SPEX Fluorolog-2 spectrofluorometer in specially designed sample holders maintained in or over the surface of liquid nitrogen. The temperature of the sample was monitored with a thermocouple sensor (Barnant Co.). The fluorescence spectra of liquid samples at ambient temperatures were recorded at right angles from solutions held in a 0.5 cm rectangular cuvette. Fluorescence spectra of PChlide were recorded within the range of 575−750 nm using different wavelengths in the Soret area of the pigment spectrum for excitation (as indicated in the figures). UV excitation spectra for PChlide, NADPH, and the various proteins were recorded between 250 and 500 nm, 250 and 400 nm, and 250 and 315 nm, respectively, by collecting fluorescence at 640, 500, and 365 nm. For recording pigment fluorescence spectra, both excitation and emission monochromator bandwidths were set at ~4 nm. For recording UV excitation spectra, the bandwidth of the emission monochromator was adjusted to 10 nm. Spectra were allowed to accumulate up to eight times, or until a good signal-to-noise ratio was obtained. All spectra were corrected for the intensity of the excitation light and the sensitivity of the photomultiplier tube. Calculations of smoothed, difference, and second-derivative spectra were performed using the Statistica-5 software package (StatSoft, Inc.).

Pigment CD spectra were recorded on a Jasco700 spectropolarimeter at room temperature at wavelengths between 400 and 460 nm from samples held in a cuvette having a 10 mm optical pass. Spectra were obtained after 25−49 accumulations at a bandwidth of 2.0 nm and speed of 100 nm/min. MV- and DV-PChlides were identified by the position of the maxima in their fluorescence excitation spectra in acetone (432 and 443 nm and 438 and 448 nm, respectively) (*28*, *29*), and the C13(2)-*R* and C13(2)-*S* stereoisomers were identified by the sign of these bands in their CD spectra (*7*) (Figure 2).

Fluorescence Estimation of Substrate and Cofactor Binding to POR. Two methods were used to assess pigment binding to POR: an increase in pigment fluorescence quantum yield following binding to the protein and the appearance of aromatic amino acid bands in the pigment fluorescence excitation spectrum due to resonance energy transfer from protein to pigment. To estimate the changes in spectra and fluorescence quantum yield in the course of PChlide binding to POR, solutions containing buffer and pigment were equilibrated in the dark at 25 °C for 3 min and the fluorescence was measured. Aliquots of recombinant POR protein solutions were then added to the sample; the solutions were allowed to equilibrate for 1 min, and fluorescence was recorded. Binding of cofactors to POR was assayed by monitoring either quenching of the protein intrinsic fluorescence or increases in NADPH fluorescence in the presence of increasing concentrations of ligand. In protein monitoring experiments, fluorescence was excited at 290 nm and emission collected at 345 nm. In cofactor monitoring experiments, NADPH and NADH fluorescence was excited at 345 nm and emission collected at 465 nm. In control experiments, aliquots of a Trp solution of the same optical density were added instead of the POR protein. This titration curve was used to calculate background fluorescence and the inner filter effect. An alternative approach to calculating the inner filter effect was based on the estimation of the sample optical density at the excitation and emission wavelengths. The cofactor concentrations were determined from their absorption spectra using extinction coefficients of 6.22 mM^{-1} cm^{-1} at 340 nm for NADPH and NADH and 18 mM^{-1} cm^{-1} at 260 nm for $NADP^+$ (*30*−*33*). For estimation of PChlide concentrations in ether solutions, the following extinction coefficients were used: 325 mM^{-1} cm^{-1} at 432 nm and 40 mM^{-1} cm^{-1} at 623 nm (*28*, *29*). Protein concentrations in the samples were assayed as described by Essen (*26*).

Calculation of ligand dissociation constants was based on the following model:

$$E + L \Leftrightarrow EL$$

which under steady-state conditions leads to the equation

$$k_2[EL] = k_1[E][L] \quad (1)$$

where [E] is the steady-state enzyme concentration, [L] is the steady-state ligand concentration, and [EL] is the steady-state concentration of the enzyme−ligand complex. k_1 and k_2 are the second-order association and first-order dissociation constants, respectively.

Assuming for the ligand titration experiment at a constant [E] that the free ligand concentration in the steady state is proportional to the fraction in the fluorescence changes:

$$[L] = [(F - F_2)/(F_1 - F_2)][Li]$$

where F is the observed fluorescence yield, F_1 and F_2 are the fluorescence yields of the pure ligand and pure ligand−enzyme complex, respectively, and [Li] is the total amount of the ligand in the sample.

If we define dissociation constant K_d as k_2/k_1, eq 1 can be expressed in the experimentally detectable values:

$$dF = dF_{max} - K_d(dF/[Li]) \text{ or}$$
$$dF/dF_{max} = [Li]/(K_d + [Li]) \quad (2)$$

where $dF = F - F_2$ and $dF_{max} = F_1 - F_2$.

Analogous equations were drawn for the E titration experiment with a constant concentration of the ligand. Estimations of K_d were made by fitting the experimental data to eq 2 at different ligand concentrations. Usually, 10−15 different concentrations of the ligand were used in each of the three sets of experiments.

Kinetic Analysis of POR Denaturation. To estimate the effects of substitutions at Tyr275 and Lys279 on POR stability in solution, we analyzed the kinetics of protein denaturation at 25 °C in the presence of 0.1% Triton X-100. In these experiments, the reaction buffer was equilibrated

to the desired temperature in the fluorometer cell and then POR was added from a stock protein solution. The kinetic data were collected using a multiwavelength program recording fluorescence at four different pairs of wavelengths (E256F500 and E288F500 for assaying changes in protein fluorescence; E340F500 and E408F500 used as a blank) with an acquisition time of 5 s and a step of 1 min. The samples were kept in the dark between the assays.

To describe a denaturation reaction consisting of two monomolecular irreversible steps (i.e., A → B → C), we used the following set of equations:

$$d[A]/dt = -k_1[A] \quad (3)$$

$$d[B]/dt = k_1[A] - k_2[B]$$

$$d[C]/dt = k_2[B]$$

$$C_{max} = A_0$$

that leads to the dependency of the accumulation of the final product with time as

$$[C]/C_{max} = 1 + [k_1 \exp(-k_2 t) - k_2 \exp(-k_1 t)]/(k_2 - k_1) \quad (4)$$

where k_1 and k_2 are the rate constants of the first and second steps of the reaction, respectively, [C] is the concentration of the final product at time t, C_{max} is the concentration of the final product after completion of the reaction, and A_0 is the initial concentration of POR.

Kinetic Analysis of Protochlorophyllide Photoconversion at Low Temperatures and Estimation of the Activation Energy of the Reaction. In our experiments, actinic light intensity was measured using a Li-Cor LI-250 light meter equipped with a LI-190SA quantum sensor. The light intensity was adjusted as necessary with neutral density glass filters.

To study the PChlide photoreduction reaction at sub-zero temperatures, samples were maintained on the sample holder, quickly frozen in liquid nitrogen, and then heated to the desired temperature in the spectrofluorometer sample compartment in the dark. To drive photoconversion, the sample was illuminated at the experimental temperature with weak monochromatic light (452 nm, 75 μE m^{-2} s^{-1}). The actinic light was used simultaneously for fluorescence excitation, and fluorescence was recorded at 644 or 685 nm with the step and integration time equal to 0.5 s. The observed fluorescence changes had two components, one fast and the other slow. The fast component exhibited a decrease in fluorescence at 644 nm and an increase in fluorescence at 685 nm. The slow component (which in our experiments does not exceed 5% of the total pigment fluorescence) exhibited a constant decline at both wavelengths. This component also occurred in samples without POR and was assigned to pigment photodegradation (*23*). For identification of the rate of PChlide photoreduction, the slow component was subtracted from the kinetic curves. The rate constant of the reaction was calculated using the least-squares fitting of experimental data at the two wavelengths with monoexponential curves. In our experiments, the contribution of the tail of the 646 nm fluorescence band in the emission at 685 nm exhibited less than 10% of the intensity of the 685 nm band and was not taken into account in our calculations. The following equations were used for our calculations, assuming that fluorescence of a reactant is proportional to its concentration and the fluorescence quantum yields of the photoactive state and the fluorescence intermediate do not change in the course of the reaction:

$$d[P]/dt = k[P]t \quad (5)$$

that leads to

$$F = F_{max} \exp(-kt) \quad (6)$$

where t is time, F is the fluorescence of the photoactive state at time t, F_{max} is its initial fluorescence at time 0, and k is the rate constant of the reaction.

Activation energy was calculated from the following equation. The reaction was performed at different temperatures, and rate constants were compared using the Boltzmann equation

$$\ln k = \ln k_0 - E_a/RT \quad (7)$$

after presentation of the results in an Arrhenius plot:

$$\log(k_2/k_1) = E_a(1/T_1 - 1/T_2)/(2.3R) \quad (8)$$

where k_1 and k_2 are rate constants at temperatures T_1 and T_2, respectively, E_a is the activation energy between temperatures T_2 and T_1, and R is the gas constant (1.987 cal mol^{-1} deg^{-1}).

Estimation of the reaction constants for all of the processes described above was performed by nonlinear regression analysis using the Statistica-5 software package.

RESULTS

Previous studies of POR activity have not taken into account the possible confounding effects that can occur as a result of the presence of different stereoisomers and derivatives of PChlide in etiolated plants (*34*), despite the fact that it has been shown that they have different spectra, different binding properties, and different photochemical activities (*7*, *8*, *29*). To exclude any possible uncertainty due to pigment complexity in the interpretation of our results, C8-ethyl-C13(2)-(*R*-)-PChlide (MV-PChlide) obtained in fraction 4 by HPLC (Figure 2) was used exclusively as the substrate in our experiments. In addition, to eliminate any possible effects on enzyme function due to steric hindrance or altered charge properties created by working with fusion proteins, the recombinant POR used in this study was devoid of MBP or His tags. We believe that these two improvements considerably enhance our ability to accurately access pigment and cofactor binding, as well as associated changes in enzyme conformation during ternary complex formation and progress through the reaction sequence.

Formation of the Photoactive State Having Fluorescence at 646 nm Is Severely Compromised in POR Proteins with Substitutions at Tyr275 and Lys279. Three discrete fluorescence bands having specific fluorescence excitation spectra were detected in frozen solutions of MV-PChlide in buffer. Their emission maxima were at 627, 633, and 638 nm. The position of the maximum of these bands depends on the chemical composition of the solvent in which the pigment is suspended, indicating that they are due to pigment−solvent interaction. Similar fluorescence bands, with excitation

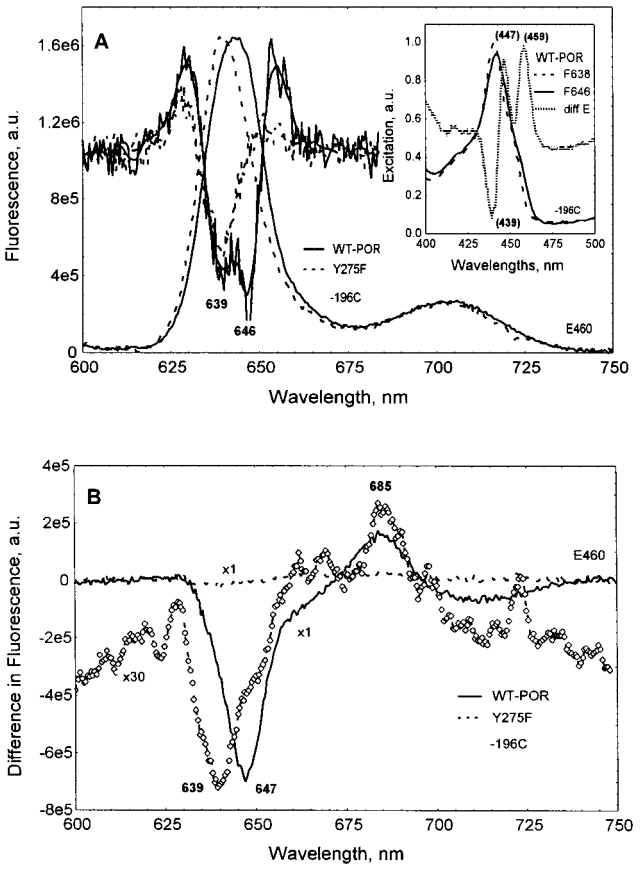

FIGURE 3: Fluorescence spectroscopic identification of the photoactive state of the NADPH−PChlide−POR ternary complex in WT and Y275F mutant pea POR. (A) Low-temperature fluorescence emission spectra and the second derivative recorded for dark-adapted samples containing 20 nM PChlide, 4 μM NADPH, and 100 nM WT POR (—) or 75 nM Y275F POR (- - -). The inset of panel A shows the excitation spectra for fluorescence at 638 and 646 nm and the difference spectrum between them for WT POR. (B) Changes in the fluorescence emissions of the same samples shown in panel A following illumination with weak monochromatic light (452 nm, 75 μE m^{-2} s^{-1}) at −50 °C for 5 min. The difference spectrum for samples containing the Y275F mutant POR is shown at two amplifications (×1 and ×30). Note that the emission at 646 nm is resolved as a separate band in the second derivative of the fluorescence spectra. Its intensity is sensitive to the presence of Tyr275 in the enzyme; it specifically disappears under illumination at low temperatures with formation of a new band at 685 nm, and it has its own excitation spectrum with bands shifted to the long wavelengths and having increased half-widths. The spectra were recorded at −196 °C. The excitation wavelength was 460 nm.

spectra shifted 5−6 nm to the long wavelengths, were detected for C8-vinyl-C13(2)-(*R*)-PChlide (data not shown).

When POR and NADPH were added to the MV-PChlide solutions and the reaction mixture was incubated in the dark at room temperature for 5 min, a new band appeared in the low-temperature fluorescence spectrum at 646 nm. This band overlaps considerably with the 638 nm band in the spectrum, but can be clearly distinguished from the latter in the second derivative of the spectrum (Figure 3A). In addition, the excitation spectrum of this band was shifted toward longer wavelengths compared to that for fluorescence at 638 nm (Figure 3A, inset), indicating that the interaction occurs before photoexcitation. Illumination of the sample at −50 °C led to a specific disappearance of this band and accumulation of a new one at 685 nm (Figure 3B). Similar phototransformations were previously detected for PORb ternary complexes in vitro and in light-adapted plants (*1*, *23*, *27*).

Mutant POR proteins with substitutions at Tyr275 and Lys279 (designated Y275F, K279I, and K279R) were previously shown to be incapable of PChlide photoreduction (*15*). The basis for this defect was not known. When we analyzed the fluorescence emission spectra of complexes formed by these mutant enzymes, no strong band at 646 nm was detected in the dark-adapted samples, indicating a dramatic reduction in their ability to form the photoactive state. Nevertheless, analysis of the second derivative of the pigment fluorescence spectra allowed us to see the appearance of a band at 646 nm after equilibration with the mutant proteins (Figure 3A). Illumination of the samples at −50 °C showed severe suppression of primary photochemical activity in the mutant proteins compared to that in WT. Nevertheless, light−dark difference spectra of the samples containing the mutant enzymes demonstrated that the formation of the 685 nm band corresponding to the fluorescence intermediate occurred at the expense of the 646 nm band (Figure 3B). The results of these two experiments demonstrate that the formation of the photoactive state and its photoconversion can be achieved in POR after substitution of Tyr275 and Lys279; however, the efficiency of photoactive state formation is decreased dramatically in the mutants. In addition to the photoinduced conversion of the PChlide fluorescence band at 646 nm, the light−dark experiments performed with the mutant enzymes also showed a decrease in the intensity of the PChlide band at 638 nm (Figure 3B). The latter effect was observed following illumination of pigment solutions in the absence of POR (data not shown) and therefore was not specific to the enzyme. The dependence of the rate of decease in the 638 nm band on the presence of dissolved oxygen suggests that this effect might be due to PChlide photooxidation (*23*).

Tyr275 and Lys279 Substitutions Do Not Block Binding of PChlide to POR. Three possible reasons can be put forth to explain the decrease in the efficiency of the formation of the photoactive state and photochemical activity of Tyr275 and Lys279 substitution mutants compared to that of WT POR: decreased affinity of mutant POR for the pigment, decreased affinity of mutant POR for NADPH, or a lowered probability of formation of the photoactive state itself. It is generally assumed that the formation of the POR photoactive state results simply from pigment and NADPH binding to the enzyme (*35*−*38*). The possibility of molecular rearrangements of the components in the ternary complex has not been considered. Since spectroscopic methods for studying PChlide binding to POR were not available, we developed two different procedures for analyzing the possible effects of PChlide interaction with WT POR. First, we studied the changes in pigment intrinsic fluorescence spectra and quantum yield upon its binding to POR. Our experiments showed that when PChlide is dissolved in Tris buffer, the pigment fluorescence intensity (excitation at 440 nm and emission at 640 nm) is low. Addition of POR protein to the solution of dissolved pigment led to an approximately 10-fold increase in pigment fluorescence quantum yield without changes in the pigment fluorescence spectrum (Figure 4A). This would account for the effect of the pigment−protein interaction.

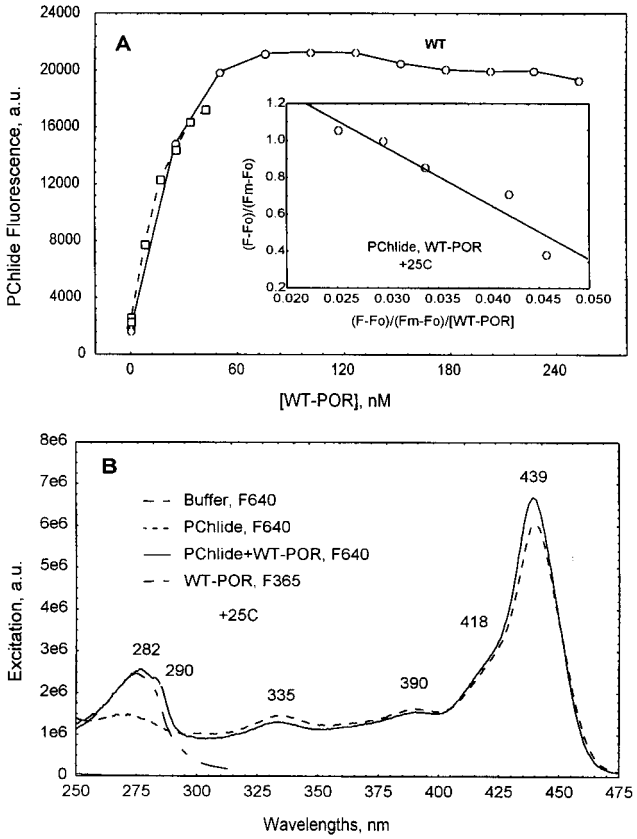

FIGURE 4: Identification of PChlide binding to POR by analysis of the changes in pigment fluorescence quantum yield in the presence of increasing amounts of the protein and by fluorescence resonance energy transfer from POR to PChlide. (A) Titration curve for the fluorescence of 20 nM chromatographically pure MV-C13(2)(*R*)-PChlide dissolved in assay buffer by the addition of either 25 (○) or 8 nM WT POR protein (□). The pigment fluorescence was monitored under excitation at 440 nm and emission at 640 nm. The inset of panel A shows data for the initial increase in the fluorescence presented in $(F - F_o)/(F_m - F_o)$ vs $(F - F_o)/(F_m - F_o)/[L]$ coordinates. (B) UV excitation spectra of fluorescence of 100 nM PChlide (emission at 640 nm) recorded before (- - -) and after (—) addition of 100 nM WT POR. Excitation spectra for intrinsic WT POR protein fluorescence (collected at 350 nm) (-·-) and for the reaction buffer (collected at 640 nm) (— — —) are shown for comparison. The intensities of the protein bands in excitation spectra were adjusted at 275 nm. All experiments were performed at 25 °C.

To confirm that the observed changes in PChlide fluorescence intensity are due to binding of PChlide to POR, we developed a second, more specific method of analysis. In this approach, we assumed that association of the pigment and protein would allow for resonance energy transfer from aromatic amino acids of the protein to the pigment. If it were true, it should lead to the appearance of aromatic amino acid bands in the pigment fluorescence excitation spectrum. This process of energy transfer can be described by the inductive-resonance mechanism developed by Forster (*39*). Three factors must be fulfilled to allow energy transfer to occur. First, the acceptor molecule (PChlide) must have absorbance in the area of the donor (protein) fluorescence. Second, the distance between the donor and acceptor must be short. For most of the known aromatic molecules, this is about 30−50 Å (*39*). Finally, the orientation of donor and acceptor electronic transition moments must have a common component.

When PChlide is dissolved in Tris buffer, no specific bands in the protein absorption area of the spectrum (250−300 nm) were detected, but the pigment had a broad continuous absorption (Figure 4B). After addition of POR to the pigment solution, three new strong bands with maxima at 277, 282, and 290 nm appeared in PChlide excitation spectra when fluorescence was collected at 640 nm (Figure 4B). Similar bands belonging to tyrosine and tryptophan (*40*) are observed in the excitation spectrum of POR protein fluorescence when fluorescence is collected at 365 nm (Figure 4B). (To exclude a possible artifact of reabsorption of the protein fluorescence by the pigment, in these experiments the optical density of the samples was adjusted to be <0.05 at 280 nm.) When similar experiments were performed with mutant PORs containing substitutions at Tyr275 and Lys279 (i.e., Y275F, K279R, or K279I), clearly recognizable protein bands were observed in the PChlide excitation spectra.

To compare the efficiency of PChlide binding to WT and mutant POR proteins, we analyzed changes in the pigment fluorescence intensity at different enzyme concentrations and calculated the respective pigment dissociation constants (K_d). In these experiments, 0.02 μM PChlide in Tris-buffered solutions was equilibrated at 25 °C in the dark for 3 min, and the pigment fluorescence excitation spectra were determined. The solutions were then titrated with aliquots of 0.01 μM POR, and the PChlide fluorescence intensity was measured after each addition of the enzyme (Figure 4A). Table 1 summarizes the estimated K_ds of PChlide binding to POR. In general, the K_ds for both the WT and mutant PORs are extremely low and of similar magnitude, indicating a high efficiency for pigment binding to the proteins. This result is consistent with the reported high-affinity binding of PChlide to barley POR estimated by gel-filtration chromatography (*41*). In our study, we also estimated the K_m for PChlide from the dependence of WT POR catalytic activity on pigment concentration (Table 1). The K_m was of the same order of magnitude as the K_d for PChlide and WT POR, although the absolute value was approximately 6-fold higher. This observation indicates that not only binding but also other factors might be involved in controlling the enzyme catalytic mechanism. One possible explanation for this difference is a change in the conformation of the ternary complex after binding of pigment and NADPH to POR has occurred. The existence of such a conformational change would be consistent with our spectroscopic data indicating formation of a specific enzyme photoactive state after substrate and cofactor binding. In general, the observed similarity in pigment K_ds obtained for WT and mutant PORs led us to conclude that the decrease in the efficiency of the formation of the enzyme photoactive state after substitution of Y275 or K279 is not due to a defect in pigment binding.

Tyr275 and Lys279 Substitutions Do Not Prevent POR from Binding NADPH, but Make the Protein More Stable against Denaturation. To estimate the efficiency of NADPH, NADH, and $NADP^+$ binding to POR, we analyzed the quenching of the protein intrinsic fluorescence following the addition of the different cofactors (*30*, *31*). In these experiments, a protein solution containing 1.6 μM WT POR in Tris assay buffer was equilibrated at 25 °C in the dark for 3 min. The protein fluorescence intensity was determined, and the reaction mixture was then titrated by the sequential addition of aliquots of one of the three cofactors. After each

Table 1: Kinetic Parameters of WT and Tyr275 and Lys279 Mutants of Pea POR

enzyme	K_d for PChlide−POR[a] (μM)	K_m for Pchlide (μM)	K_d for POR−NADPH[b] (μM)	K_d for NADPH−POR[c] (μM)	K_m for NADPH (μM)	k_1 for POR denaturation (s^{-1})	k_2 for POR denaturation (s^{-1})	reaction yield at 25 °C (%)	reaction yield at −50 °C (%)
WT	0.030 ± 0.004	0.18 ± 0.02	13.0 ± 1.9	21.8 ± 2.8	11.0 ± 2.0	201.0 ± 50	4.0 ± 0.3	56 ± 6	11 ± 2
Y275F	0.050 ± 0.014	-	19.5 ± 2.3	24.9 ± 1.7	-	15.0 ± 10	3.1 ± 0.3	4.4 ± 0.5	nd[d]
K279I	0.022 ± 0.018	-	16.3 ± 3.2	68.1 ± 17.1	-	74.0 ± 25	3.0 ± 0.3	3.1 ± 0.5	nd[d]
K279R	0.027 ± 0.013	-	48.2 ± 5.2'	42.1 ± 5.5	-	30.8 ± 16	2.8 ± 0.3	0.0 ± 0.5	nd[d]

[a] Determined from changes in pigment fluorescence in the presence of various amounts of the protein. [b] Determined from changes in protein fluorescence in the presence of various amounts of NADPH. [c] Determined from changes in NADPH fluorescence in the presence of various amounts of NADPH. [d] Not determined.

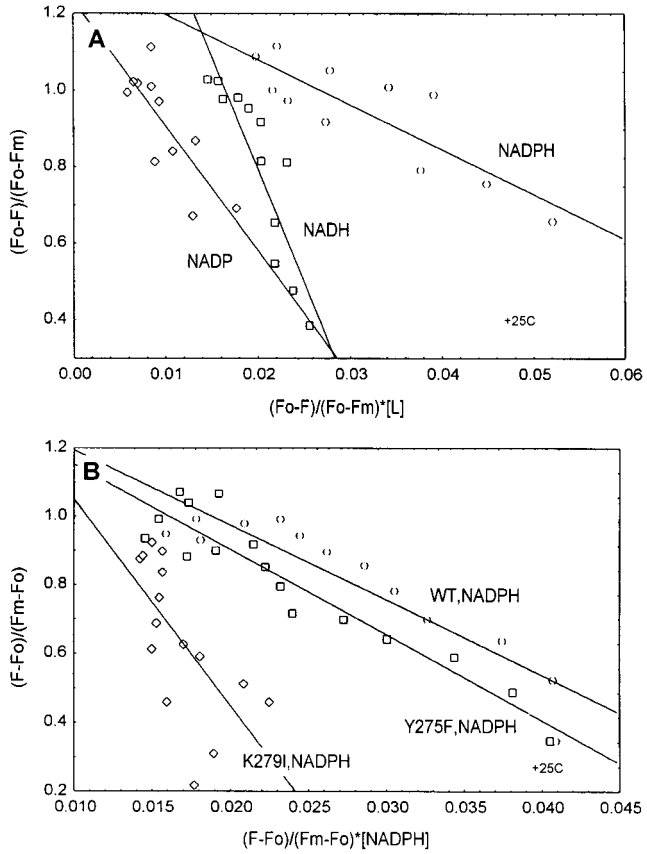

FIGURE 5: Estimation of the efficiency of NADPH, NADH, and $NADP^+$ binding to POR determined by analysis of quenching of the intrinsic protein fluorescence and activation of NADPH fluorescence in the presence of increasing amounts of ligands. (A) Changes in intrinsic protein fluorescence of WT POR (170 nM) titrated with 4 μM NADPH, 5 μM NADH, or 12.4 μM $NADP^+$. The protein titration data are presented in $(F_o - F)/(F_o - F_m)$ vs $(F_o - F)/(F_o - F_m)/[L]$ coordinates. Protein fluorescence was monitored under excitation at 290 nm and emission at 345 nm. All titration experiments were performed at 25 °C. (B) Changes in NADPH fluorescence measured in reaction mixtures containing 2.53 μM WT POR, 1.96 μM Y275F, or 1.68 μM K279I POR to which NADPH was added at a concentration of 4 μM/step. The NADPH titration data are presented in $(F - F_o)/(F_m - F_o)$ vs $(F - F_o)/(F_m - F_o)/[NADPH]$ coordinates. NADPH fluorescence was excited at 345 nm and collected at 465 nm. All titration experiments were performed at 25 °C.

addition of cofactor, the POR fluorescence was measured. The titration curves and K_ds resulting from these studies are shown in Figure 5A. The K_d for NADH was ~5-fold higher than the value observed for NADPH, consistent with the known specificity of POR for NADPH. The observed higher K_d for $NADP^+$ compared to that for NADPH indicates repulsion of the oxidized cofactor from POR. Similar results were obtained when we estimated K_ds for NADPH binding to POR by measuring an increase in NADPH fluorescence (Figure 5B). Overall, the K_ds observed for POR were comparable to those observed for other short chain dehydrogenases/reductases (*30*, *31*).

The cofactor dissociation constants measured for recombinant WT pea POR obtained in the above experiments using two independent approaches (i.e., titration of protein fluorescence and titration of NADPH fluorescence) differ considerably from those reported for recombinant WT POR from *Synechocystis* (*21*). The reason for this difference is not clear, but might reflect the origin of the protein, the presence of a His tag on the bacterial enzyme, or the presence of detergent micelles in the assay solution. Moreover, the K_d for the WT pea POR measured in our study coincides well with the K_m estimated for the same protein (Table 1) and with K_d values estimated for other POR proteins isolated from different organisms (*2*, *19*). In general, the K_ds for the cofactor determined for the various mutant PORs were comparable, with some variation. The lowest values were obtained for WT and the Y275F mutant, whereas the highest K_d was found for K279R (Table 1). Taken together, these data suggest that while substitutions at Tyr275 and Lys279 do not prevent NADPH binding to the enzyme, they contribute to the loss of catalytic function in a yet to be determined manner.

In an attempt to identify the role of Tyr275 and Lys279 in stabilization of POR, we studied the kinetics of protein denaturation at ambient temperature in the absence of substrate and cofactor. Preliminary studies had shown that the loss of POR catalytic activity is correlated with an increase in enzyme fluorescence monitored at 500 nm. The remarkable feature of this increase was that it had an S shape, but was not exponential as might be expected for a monomolecular reaction (Figure 6). The S shape of the curve indicates that the process consists of at least two sequential steps or has a cooperative character (*42*, *43*). To approach the mechanism of the denaturation process, we tested kinetic models for monomolecular, two sequential monomolecular, bimolecular, and monomolecular cooperative reactions to fit experimental curves using least-squares nonlinear regression analysis. The best results for WT POR and the Y275F mutant were obtained with the model of two sequential monomolecular reactions. For the K279I and K279R mutants, the shapes of the curves were more complex, indicating two parallel two-step processes (Figure 6). Assuming that two sequential irreversible monomolecular reactions determine the rate of the process (see Materials and Methods), we calculated their rates from the kinetics of the fluorescence changes in WT and mutant POR at 25 °C (Table 1). The

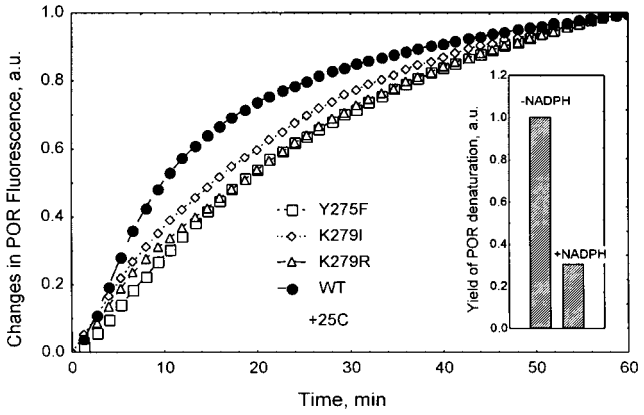

FIGURE 6: Time course of POR denaturation measured in reaction mixtures containing POR protein (100 nM WT, 55 nM Y275F, 74 nM Y279, or 81 nM Y279R POR) and 0.1% Triton X-100 at 25 °C. Increases in fluorescence were monitored at 500 nm under excitation at 280 nm. The changes were normalized to 1 after 1 h. The inset shows the relative amounts of denaturated WT POR, in the absence (−NADPH) and presence (+NADPH) of 1 μM NADPH during denaturation in the dark for 1 h at 25 °C.

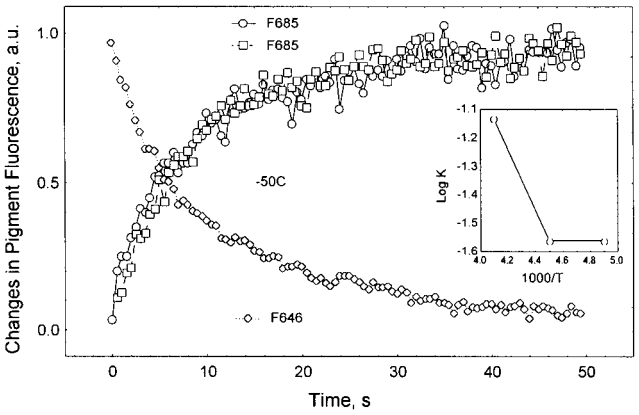

FIGURE 7: Time course of the photoconversion of the WT POR photoactive state (detected by fluorescence at 646 nm) and the formation of the fluorescence intermediate (detected by fluorescence at 685 nm) under illumination of a dark-adapted frozen sample containing 4 μM NADPH, 20 nM PChlide, and 100 nM WT POR with monochromatic blue light (452 nm, 75 μE m^{-2} s^{-1}) at −50 °C. The time course of the changes in fluorescence at 685 nm is shown for two independent experiments. The inset shows an Arrhenius plot (log K vs 1/T) for the reaction at three different temperatures (−70, −50, and −30 °C).

rates of the slow step of the reaction were highest for the WT and subsequently decrease in the following order for the POR substitution mutants: WT > Y275F > K279I > K279R. Thus, even in the absence of substrate and cofactor, WT POR appears to adopt a thermodynamically unfavorable conformation with Tyr275 or Lys279 contributing to the destabilization of the enzyme. When we checked the effect of adding saturating amounts of NADPH on denaturation of WT POR, we observed an approximately 3-fold decrease in the denaturation yield (Figure 6, inset), indicating a possible protective role of the cofactor.

Tyr275 Substitution Specifically Inactivates the Second (Light-Independent) Step of the PChlide Photoreduction Reaction. We previously reported that the PChlide photoreduction reaction catalyzed by barley PORb in vitro consists of two steps with the formation of an unstable reaction intermediate with a fluorescence maximum at 685 nm separating the two steps (*23*). The same two-step reaction was detected with WT pea POR. To assay the first, light-dependent step of PChlide photoreduction, we studied the kinetics of the conversion of the photoactive state into the 685 nm intermediate by WT POR at different sub-zero temperatures. In these experiments, a ternary complex was assembled in the dark at room temperature. The samples were then frozen to −196 °C, heated in the dark to −70, −50, or −30 °C, and illuminated at these temperatures with monochromatic 452 nm blue light (80 μE m^{-2} s^{-1}). The kinetics of the disappearance of the photoactive state and accumulation of the intermediate were monitored at 646 and 685 nm, respectively. At the light intensity and temperatures that were tested, the kinetics of the reaction at both wavelengths were well described by monoexponential curves. The deviation of the experimental points from the monoexponential law was not more than 5%. Calculated rate constants for the disappearance of the F646 species and accumulation of the F685 form were nearly identical (approximately 0.12 s^{-1}) (Figure 7), indicating direct interconversion of the photoactive state and the intermediate. Comparison of the reaction at different temperatures showed that the rate constants of the reaction were about the same at −70 and −50 °C, but increased 5-fold at −30 °C (Figure 7, inset). On the basis of this difference, the activation energy of the reaction between each pair of temperatures was estimated to be approximately 8.17 kcal mol^{-1} between −50 and −30 °C and approximately 0 kcal mol^{-1} between −70 and −50 °C. The presence of two different activation energies indicates two different reaction mechanisms at the two temperature ranges. Close to zero activation energy more likely indicates tunneling hydrogen transfer (*39*). The activation energy observed in the −50 to −30 °C temperature range is more typical of mechanisms involving hydrogen abstraction (*39*), or photoisomerization (*23*).

The low intensity of the F646 fluorescence bands in the POR mutants does not allow for precise determination of the kinetics of their photoconversion at low temperatures. To identify the step where the enzymatic reaction could be inactivated in these mutant enzymes, we illuminated the samples at 25 °C with continuous white light (30 μE m^{-2} s^{-1}) for 10 min. In the WT POR, this treatment led to the accumulation of the final product (Chlide) with a fluorescence maximum at 675 nm. With the mutant PORs, we observed nearly no photochemical activity. Nevertheless, when we assayed fluorescence at −196 °C, we found that the Y275F mutant initiated photoconversion of the substrate, but produced only the F682 intermediate (Figure 8). The K279I mutant catalyzed the formation of a mixture of 685 and 675 nm bands, resulting in the accumulation of a broad emission band with a maximum at 678 nm. No formation of any new band was detected following illumination of reaction mixtures containing the K279R mutant (Figure 8). Despite the considerable decrease in the intensities of the fluorescence bands accumulated in the mutants at room temperature, the band intensities observed in reactions involving the mutant PORs were comparable to those observed with WT POR at −50 °C (Table 1) where the reaction does not proceed beyond the formation of the F685 intermediate (*23*). Both the spectroscopic features and intensities of the fluorescence bands indicate that POR mutants containing substitutions in Tyr275 stop their reaction sequence after formation of the F685 intermediate. Substitu-

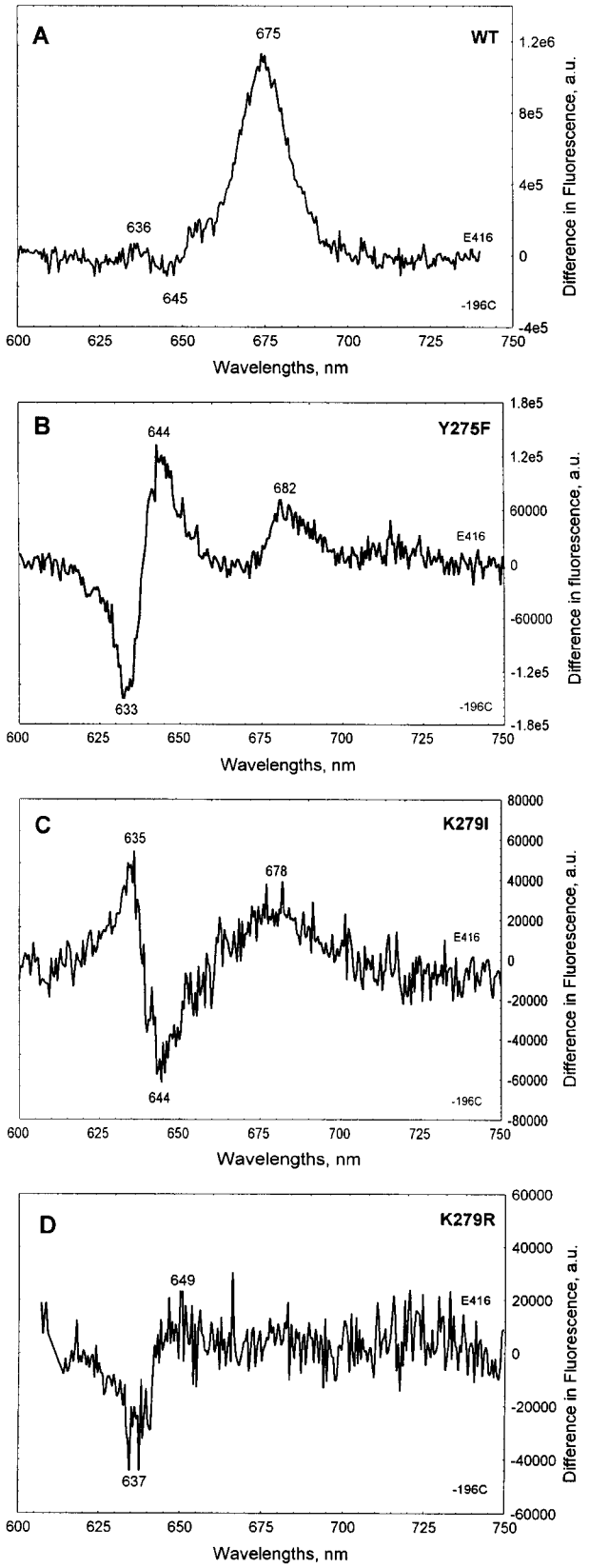

FIGURE 8: Fluorescence spectroscopic characterization of the reaction products formed by WT and mutant POR proteins. Shown are the fluorescence spectra of the reaction products formed by (A) 100 nM WT POR, (B) 55 nM Y275F POR, (C) 74 nM Y279I POR, and (D) 81 nM Y279R POR in the presence of 4 μM NADPH and 100 nM Pchlide. The fluorescence spectra were recorded at −196 °C under excitation at 416 nm before and after illumination of the samples with white light (33 μE m^{-2} s^{-1}) at 25 °C for 10 min. The spectra were normalized at 640 nm before subtraction.

tion of Lys279 leads to either complete inactivation of the enzyme (as is the case with the K279R mutant) or formation of an enzyme that can carry out the photoreduction reaction to the end, but with a very low yield (as observed with the K279I mutant).

In addition to the photochemical activity resulting in the formation of the fluorescence band at 685 nm, illumination at room temperature of the complexes formed by the mutant POR, as well as those formed by the WT enzyme, leads to a wavelength shift of the main PChlide fluorescence band. This shift was detected in all mutants, including K279R. The shift was toward short wavelengths in the WT POR and K279I mutant, but toward longer wavelengths in the Y275F and K279R mutants (Figure 8). This shift might indicate that polarization of the microenvironment after the extent of pigment photoexcitation is determined by the nature of the local amino acids.

DISCUSSION

Two families of NADPH-requiring enzymes (oxidoreductases) have been identified on the basis of their protein sequence similarities: aldoketoreductases (AKR) and short chain dehydrogenases/reductases (SDR). Despite the fact that both families utilize NADPH, individual members of the two families differ from each other in the enzyme folding, reaction stereochemical course, and catalytic mechanism. The AKR family includes ~20 known members (*44*). The enzymes of this group usually form β-barrel structures, are monomeric, and utilize the 4*R*-hydrogen of NADPH leading to their designation as A-side dehydrogenases. The SDR family has ~60 known members (*16*). X-ray crystallographic and NMR analysis of the ternary (3D) structure of members of this family revealed an $\alpha-\beta-\alpha$ sandwich, composed of approximately five β-strands assembled in a β-sheet. The enzymes in this family frequently form homodimers or homotetramers, have a conserved $\beta-\alpha-\beta$ fold for NADPH binding, and utilize the 4*S*-hydrogen of the cofactor in the course of the reaction. These enzymes are termed B-side dehydrogenases. In almost all of the enzymes, the conserved $\beta-\alpha-\beta$ fold for NADPH binding is located at the N-terminus of the enzyme. In contrast, the C-terminal portion of the enzyme, thought to be involved in substrate binding, is considerably more variable. Another typical feature of SDR family members is the presence of a signature pentapeptide sequence within the catalytic site consisting of absolutely conserved Tyr and Lys residues separated by three amino acids (Tyr-X-X-X-Lys) (*17*, *18*). On the basis of protein sequence similarity, the presence of the conserved Tyr-X-X-X-Lys pentapetide motif (*15*), and utilization of the pro-*S*-hydrogen of NADPH in catalysis (*4*), POR was identified as a member of SDR family (*15*).

Two main features distinguish POR from other members of the SDR family (and most other enzymes). These are utilization of a porphyrin as a substrate and the strict light dependency of enzyme activity. In the study presented here, we took advantage of both these features. The unique spectral properties of porphyrins allowed us to directly use the substrate as an internal fluorescence probe in studies of the enzyme's structure, whereas the strict dependency of the enzyme on light allowed us to use light as a trigger to control the progress of the reaction.

In our previous studies (*23*), we identified the main steps of the POR-catalyzed PChlide photoreduction reaction in vitro by following the temperature dependence of light-induced changes in PChlide fluorescence. These studies established a reaction sequence in which formation of the photoactive state of the POR−NADPH− PChlide ternary complex having a fluorescence at 646 nm is followed by light-induced conversion of the photoactive complex into an unstable F685 intermediate and subsequent dark relaxation to the state fluorescing at 675 nm.

In this work, we demonstrated that Tyr275 and Lys279 of POR, corresponding to the two highly conserved catalytic site amino acids found in all SDR family members, are not crucial for substrate and cofactor binding, but are necessary for the formation of the enzyme photoactive state. In members of the SDR family for which a 3D structure has been determined, it has been shown that the conserved Tyr and Lys residues are involved in stabilization of the nicotinamide portion of NADPH by coordination of its ribose moiety (PDB entry 1CYD, GenBank accession number P08074). Our experiments with POR show that the presence of Tyr275 and Lys279 shifts the enzyme into a thermodynamically unfavorable configuration (indicated by the 3−10-fold increase in the enzyme denaturation rate) and leads to a dramatic (10−20-fold) increase in catalytic activity. Following substitution of Tyr275 and Lys279, formation of the photoactive state is still possible in the mutant POR proteins; however, the probability of finding the enzyme in this state is considerably lower.

Protein modeling studies with POR (*1*, *14*) indicate that both Tyr275 and Lys279 are located close to the hydrophobic core of the enzyme. Substitution of Phe for Tyr (e.g., Y275F POR) does not change the charge or steric volume of the amino acid residue, but increases the hydrophobicity and prevents the formation of a salt bridge by the enzyme at this position. The increase in hydrophobicity or the reduction of the steric volume of one of the amino acids in the enzyme should not prevent the assembly of the catalytic core. However, the inability to form a hydrogen bound can destabilize coordination of a bound molecule. Indeed, according to our data, substitution of Phe for Tyr275 considerably reduces the efficiency of the formation of the ternary complex photoactive state fluorescing at 646 nm. According to the available crystallographic data for dehydrofolyate reductase, the conserved Tyr located after the fifth β-strand is oriented to the ribose ring of the nicotinamide portion of NADPH. The other NADPH binding sites are located after the first, second, and third β-strands of the enzyme. These binding sites coordinate the phosphate bridge between the two riboses of NADPH, a phosphate group at the ribose of adenine, and adenine itself, respectively. Thus, substitutions at any one of these binding sites alone should not be sufficient to prevent NADPH binding to POR, but in the case of Tyr275 mutants could prevent exact coordination of the nicotinamide part of the molecule. Consistent with this, our data show that the probability of POR forming the photoactive state (F646) is dramatically reduced in mutants containing substitutions at this residue. At the same time, we did not detect a substantial decrease in the ability of the mutant enzyme to bind substrate or cofactor compared to that of the WT POR.

Despite the reduction in the fluorescence intensity at 646 nm, the Y275F mutant performs the initial photochemical step, suggesting that substitution at Tyr275 decreases the probability of achieving the photoactive state, but does not completely block the photoreduction reaction. In addition, our spectroscopic analysis revealed that in the mutant PORs the photoreduction reaction does not proceed beyond the formation of the F685 intermediate even at room temperature.

The effects of substitutions at Lys279 are more complex. Substituting Ile for Lys279 does not change the amino acid volume, but increases the local hydrophobicity. In addition, Ile is not charged and does not form a salt bridge. As in the case of POR mutants with Tyr275 substitutions, K279I mutants exhibited a dramatically decreased ability to form the photoactive state and decreased catalytic activity. However, these mutants are not completely blocked in their catalytic activity. In addition, analysis of pigment fluorescence showed shifts to either longer or shorter wavelengths (depending on which Lys279 mutant was analyzed), indicating that its position is determined by local charges on the polypeptide chain near the NADPH binding site. Several hypotheses have been put forward about the origin of the PChlide photoactive state in vivo: pigment dimerization, pigment to enzyme binding, and POR aggregation (*35*−*37*). Our studies show that one of the most important factors in determining pigment spectral properties is the local charge of the protein near the catalytic site. In this respect, it is interesting to note that in this work we also detected photoinduced electrochromic polarization of the main PChlide form bound to the enzyme. Moreover, this polarization has the opposite direction in the completely inactive K279R mutant.

In contrast to the other mutant PORs examined in this study, PORs containing Arg substitutions at Lys279 not only fail to form the photoactive state but also are completely blocked in their ability to carry out the initial photochemical step of the photoreduction reaction. Substitution of Arg for Lys does not change the amino acid charge at that location in the protein or interfere with the ability to form a salt bridge. Arg has a larger steric volume and reduces the hydrophobicity. Both these factors seem to prevent NADPH from being properly inserted into the enzyme's catalytic site. Thus, POR inactivation in the K279R mutant is most likely due to an inability of NADPH to fit into the enzyme as a result of a steric problem.

If we judge from the position of the PChlide fluorescence spectrum in the photoactive state (F646) compared to free and solvated pigment (F627, F633, and F638 bands), transformation of the enzyme ternary complex into the photoactive state decreases the energy of the pigment excited state. Since a corresponding long wavelength shift is also observed in the pigment excitation spectrum, the emission at 646 nm does not belong to an exciplex (a complex formed by the pigment in a photoexcited state). Redox titration experiments indicate that this state might be the result of a specific interaction of the pigment with NADPH and/or specific amino acid residues within the POR protein. Binding of the pigment to the enzyme, which is likely a prerequisite for this spectral shift, is not enough for the formation of the photoactive state.

Several new insights into the nature of the light-dependent step of the PChlide photoreduction reaction mechanism were

provided by our analysis of the kinetics of pigment phototransformation in the WT POR. First, since both the kinetics of the disappearance of the F646 band and the accumulation of the F685 intermediate were found to have the same rate, this confirmed not only that the F646 species is photoactive but also that it directly participates in the formation of the F685 fluorescent intermediate. Second, the observed temperature dependence of the reaction between −50 and −30 °C, with an activation energy of ∼8 kcal mol^{-1}, is typical for a process involving hydrogen transfer (*39*). Third, the lack of a temperature effect on the reaction below −50 °C indicates the possible existence of a tunneling mechanism (*39*). NADPH, the primary donor of hydrogen in PChlide photoreduction, must therefore come into direct contact with the pigment in the photoactive complex fluorescing at 646 nm.

The second fundamental finding about the POR catalytic mechanism revealed in this work is that Tyr275 participates in the second, light-independent step of the PChlide reduction reaction. This is evidenced in the fact that the Y275F mutant carries out the first step of PChlide reduction at room temperature (i.e., F685 formation) but cannot complete the second step of the reaction, and Chlide F675 does not accumulate. The exact molecular process occurring during the second step of the PChlide photoreduction reaction and the role Tyr plays need to be clarified. This step might involve either enzyme isomerization (conformational change) or hydrogen transfer from Tyr275 to NADP$^+$ or to the semireduced pigment. Work is now underway in an attempt to resolve the crucial role of this residue.

In conclusion, our data demonstrate that the binding of NADPH and PChlide by POR is not sufficient for the formation of the enzyme photoactive state. Rather, formation of the photoactive state requires proper coordination of all reaction components, NADPH and PChlide, in the enzyme catalytic pocket and the active participation of Tyr275 and Lys279. Rate constants for dissociation of NADPH and PChlide from POR are very low, indicating a nearly irreversible binding of the substrate and cofactor to the enzyme in the dark. The rate and temperature dependence of the photoinduced formation of the F685 fluorescence intermediate indicates that the first step in the Pchlide photoreduction reaction mechanism involves a direct hydrogen transfer between NADPH and PChlide. In addition to being responsible for the stabilization of the cofactor and pigment in the photoactive state, Tyr275 is directly involved in the second step of PChlide photoreduction reaction, dark conversion of the F685 fluorescence intermediate into the final product, Chlide.

ACKNOWLEDGMENT

We thank Trevor Griffiths for an antiserum for wheat POR and his comments on the manuscript. We are also indebted to Steffen Reinbothe and Anthony Spano for their helpful discussions of the results throughout this investigation.

REFERENCES

1. Lebedev, N., and Timko, M. P. (1998) *Photosynth. Res. 58*, 5−23.
2. Griffiths, W. T. (1978) *Biochem. J. 174*, 681−692.
3. Oliver, R. P., and Griffiths, W. T. (1981) *Biochem. J. 195*, 93−101.
4. Valera, V., Fung, M., Wessler, A. N., and Richards, W. R. (1987) *Biochem. Biophys. Res. Commun. 148*, 515−520.
5. Begley, T. P., and Young, H. (1989) *J. Am. Chem. Soc. 111*, 3095−3096.
6. Griffiths, W. T. (1980) *Biochem. J. 186*, 267−278.
7. Helfrich, M., Schoch, S., Schafer, W., Ryberg, M., and Rudiger, W. (1996) *J. Am. Chem. Soc. 118*, 2606−2611.
8. Knaust, R., Seyfried, B., Schmidt, L., Schulz, R., and Senger, H. (1993) *J. Photochem. Photobiol., B 20*, 161−166.
9. Schoch, S., Helfrich, M., Wiktorsson, B., Sundqvist, C., Rudiger, W., and Ryberg, M. (1995) *Eur. J. Biochem. 229*, 291−298.
10. Klement, H., Helfrich, M., Oster, U., Schoch, S., and Rudiger, W. (1999) *Eur. J. Biochem. 265*, 862−874.
11. Schulz, R., Steinmuller, K., Klaas, M., Forreiter, C., Rasmussen, S., Hiller, C., and Apel, K. (1989) *Mol. Gen. Genet. 217*, 355−361.
12. Darrah, P. M., Kay, S. A., Teakle, G. R., and Griffiths, W. T. (1990) *Biochem. J. 265*, 789−798.
13. Spano, A. J., He, Z., Michel, H., Hunt, D. F., and Timko, M. P. (1992) *Plant Mol. Biol. 18*, 967−972.
14. Dahlin, C., Aronson, E., Wilks, H., Lebedev, N., Sundqvist, C., and Timko, M. P. (1999) *Plant Mol. Biol. 39*, 309−323.
15. Wilks, H. M., and Timko, M. P. (1995) *Proc. Natl. Acad. Sci. U.S.A. 92*, 724−728.
16. Jornvall, H., Persson, B., Krook, M., Arian, S., Gonzales-Duarte, R., Jeffery, J., and Ghosh, D. (1995) *Biochemistry 34*, 6003−6013.
17. Carugo, O., and Argos, P. (1997) *Proteins 28*, 10−28.
18. Luba, J., Nare, B., Liang, P. H., Anderson, K. S., Beverley, S. M., and Hardy, L. W. (1998) *Biochemistry 37*, 4093−4104.
19. Martin, G. E. M., Timko, M. P., and Wilks, H. M. (1997) *Biochem. J. 325*, 139−145.
20. Townley, H. E., Griffiths, W. T., and Nugent, J. P. (1998) *FEBS Lett. 422*, 19−22.
21. Heyes, D. J., Martin, G. E. M., Reid, R. J., Hunter, C. N., and Wilks, H. M. (2000) *FEBS Lett. 483*, 47−51.
22. Griffiths, W. T., McHugh, T., and Blankenship, R. E. (1996) *FEBS Lett. 398*, 235−238.
23. Lebedev, N., and Timko, M. P. (1999) *Proc. Natl. Acad. Sci. U.S.A. 96*, 9954−9959.
24. Sheffield, P. J., Garrard, S. M., et al. (1999) *Protein Expression Purif. 15* (1), 34−39.
25. Sambrook, J., Fritsch, E. F., and Maniatis, T. (1989) *Molecular Cloning. A Laboratory Manual*, Cold Spring Harbor Laboratory Press, Plainview, NY.
26. Esen, A. (1978) *Anal. Biochem. 89*, 264−273.
27. Lebedev, N., VanCleve, B., Armstrong, G., and Apel, K. (1995) *Plant Cell 7*, 2081−2090.
28. Houssier, C., and Sauer, K. (1968) *Biochim. Biophys. Acta 172*, 492−502.
29. Tripathy, B. C., and Rebeiz, C. A. (1985) *Anal. Biochem. 149*, 43−61.
30. Schlegel, B. P., Jez, J. M., and Penning, T. M. (1998) *Biochemistry 37*, 3538−3548.
31. Miller, G. P., and Benkovic, S. J. (1998) *Biochemistry 37*, 6327−6335.
32. Basso, L. A., Engel, P. C., and Wamsley, A. R. (1995) *Eur. J. Biochem. 234*, 603−615.
33. Basran, J., Casarotto, M. G., Basran, A., and Roberts, G. C. K. (1997) *Protein Eng. 10*, 815−826.
34. Sperling, U., Frank, F., VanCleve, B., Frick, G., Apel, K., and Armstrong, G. (1998) *Plant Cell 10*, 283−296.
35. Boddi, B., Ryberg, M., and Sundqvist, C. (1992) *J. Photochem. Photobiol., B 12*, 389−401.
36. Boddi, B., Ryberg, M., and Sundqvist, C. (1993) *J. Photochem. Photobiol., B 21*, 125−133.

37. Klement, H., Oster, U., and Rudiger, W. (2000) *FEBS Lett. 480*, 306−310.
38. Boddi, B., and Franck, F. (1998) *J. Photochem. Photobiol. B, 41*, 73−82.
39. Lakowicz, J. R. (1999) *Principles of fluorescence spectroscopy*, 2nd ed., pp 698, Kluwer Academic/Plenum, New York.
40. Houtzager, V., Ouellet, M., Falgueyret, J.-P., Passmore, L. A., Bayly, C., and Percival, M. D. (1996) *Biochemistry 35*, 10974−10984.
41. Reinbothe, S., Reinbothe, C., Neumann, D., and Apel, K. (1996) *Proc. Natl. Acad. Sci. U.S.A. 93*, 12026−12030.
42. Bollinger, J. M., Tong, W. H., Ravi, N., Huynh, H. H., Edmondsom, D. E., and Stubbe, J. (1995) in *Methods in Enzymology* (Klinman, J., Ed.) Vol. 258, pp 278−302, Academic Press, San Diego.
43. Neet, K. E. (1983) in *Contemporary Enzyme Kinetics and Mechanizm* (Purich, D. L., Ed.) pp 267−320, Academic Press, Orlando, FL.
44. Bruce, N. C., Willey, D. L., Coulson, A. F. W., and Jeffery, J. (1994) *Biochem. J. 299*, 805−811.

BI0105025